

# Large Electrically Induced Height and Volume Changes in Poly(3,4-ethylenedioxythiophene)/Poly(styrenesulfonate) Thin Films

Dimitri S. H. Charrier, René A. J. Janssen, and Martijn Kemerink\*

Department of Applied Physics, Eindhoven University of Technology, P.O. Box 513 5600,  
MB Eindhoven, The Netherlands

Received February 12, 2010. Revised Manuscript Received May 17, 2010

We demonstrate large, partly reversible height and volume changes of thin films of poly(3,4-ethylenedioxythiophene)/poly(styrenesulfonate) (PEDOT:PSS) on the anode of interdigitating gold electrodes under ambient conditions by applying an electrical bias. The height and volume changes were monitored with optical and atomic force microscopy and are found to be independent of initial film thickness. In the first cycle, a relative height change of 950% is observed for a 21 nm thick film. Two regimes are identified. In the first regime, reversible redox reactions occur and reversible height changes can be ascribed to absorption of water via osmotic effects, brought about by an increasing ion concentration on the anode. In the second, irreversible regime, irreversible overoxidation of the PEDOT occurs and mass transport from the channel to the anode becomes important.

## 1. Introduction

Poly(3,4-ethylenedioxythiophene) blended with poly(styrenesulfonate) (PEDOT:PSS)<sup>1</sup> is frequently used in organic electronics as electrode material in field-effect transistors,<sup>2,3</sup> solar cells,<sup>4</sup> and light-emitting diodes.<sup>5,6</sup> Despite its ubiquitous use, PEDOT:PSS remains a somewhat mysterious material with a highly anisotropic conductivity<sup>7,8</sup> that is a strong but ill understood function of humidity,<sup>9,10</sup> pH,<sup>11</sup> solvent,<sup>12</sup> and thermal treatment.<sup>10</sup> Also, the optical properties are anisotropic<sup>13</sup> and depend

strongly on the oxidation state of the PEDOT,<sup>14,15</sup> allowing the use in electrochromic displays.<sup>16</sup> In addition, PEDOT:PSS has been employed as active material in microfuses,<sup>17</sup> memory elements,<sup>18</sup> electrochemical logic circuits,<sup>19</sup> and in chemical and biological sensors.<sup>20</sup> In this work, we report on strong height and volume changes observed in PEDOT:PSS thin films on the anode of interdigitating gold electrodes under ambient conditions that are reminiscent of actuation.

The most widely studied  $\pi$ -conjugated polymer in organic actuators is polypyrrole (PPy). Combined with dodecylbenzenesulfonate (DBS), PPy manifests an in-plane elongation that can be converted into a bending motion on micro- or millimeter scales with long lifetimes.<sup>21</sup> The PPy: DBS system uses an additional electrolyte as an ionic reservoir, called a “wet” or “dry” actuator if the reservoir is a liquid<sup>22</sup> or a solid<sup>23</sup> ion source. Under an externally applied voltage, the mobile anions or cations present in the electrolyte can move and create a volume expansion (or contraction) in the polymer by insertion (or deinsertion) of

\*To whom correspondence should be addressed. E-mail: m.kemerink@tue.nl.

- (1) Kirchmeyer, S.; Reuter, K. *J. Mater. Chem.* **2005**, *15*, 2077.
- (2) Sirringhaus, H.; Kawase, T.; Friend, R. H.; Shimoda, T.; Inbasekaran, M.; Wu, W.; Woo, E. P. *Science* **2000**, *290*, 2123.
- (3) Touwslager, F. J.; Willard, N. P.; de Leeuw, D. M. *Appl. Phys. Lett.* **2002**, *81*, 4556.
- (4) Roman, L. S.; Mammo, W.; Pettersson, L. A. A.; Andersson, M. R.; Inganäs, O. *Adv. Mater.* **1998**, *10*, 774.
- (5) Cao, Y.; Yu, G.; Zhang, C.; Menon, R.; Heeger, A. J. *Synth. Met.* **1997**, *87*, 171.
- (6) Carter, S. A.; Angelopoulos, M.; Karg, S.; Brock, P. J.; Scott, J. C. *Appl. Phys. Lett.* **1997**, *70*, 2067.
- (7) Nardes, A. M.; Kemerink, M.; Janssen, R. A. J.; Bastiaansen, J. A. M.; Kiggen, N. M. M.; Langeveld, B. M. W.; van Breemen, A. J. J. M.; de Kok, M. M. *Adv. Mater.* **2007**, *19*, 1196.
- (8) Nardes, A. M.; Kemerink, M.; Janssen, R. A. J. *Phys. Rev. B* **2007**, *76*, 085208.
- (9) Nardes, A. M.; Kemerink, M.; de Kok, M. M.; Vinken, E.; Maturrova, K.; Janssen, R. A. J. *Org. Electron.* **2008**, *9*, 727.
- (10) Huang, J.; Miller, P. F.; Wilson, J. S.; de Mello, A. J.; de Mello, J. C.; Bradley, D. D. C. *Adv. Funct. Mater.* **2005**, *15*, 290.
- (11) Aleshin, A. N.; Williams, S. R.; Heeger, A. J. *Synth. Met.* **1998**, *94*, 173.
- (12) Kim, J. Y.; Jung, J. H.; Lee, D. E.; Joo, J. *Synth. Met.* **2002**, *126*, 311.
- (13) Pettersson, L. A. A.; Carlsson, F.; Inganäs, O.; Arwin, H. *Thin Solid Films* **1998**, *313*, 356.
- (14) Gustafsson, J. C.; Liedberg, B.; Inganäs, O. *Solid State Ionics* **1994**, *69*, 145.
- (15) Heuer, H. W.; Wehrmann, R.; Kirchmeyer, S. *Adv. Funct. Mater.* **2002**, *12*, 89.

- (16) Kumar, A.; Welsh, D. M.; Morvant, M. C.; Piroux, F.; Abboud, K. A.; Reynolds, J. R. *Chem. Mater.* **1998**, *10*, 896.
- (17) de Brito, B. C.; Smits, E. C. P.; van Hal, P. A.; Geuns, T. C. T.; de Boer, B.; Lasance, C. J. M.; Gomes, H. L.; de Leeuw, D. M. *Adv. Mater.* **2008**, *20*, 3750.
- (18) Möller, S.; Perlov, G.; Jackson, W.; Taussig, C.; Forrest, S. *Nature* **2003**, *426*, 166.
- (19) Nilsson, D.; Robinson, N.; Berggren, M.; Forchheimer, R. *Adv. Mater.* **2005**, *17*, 353.
- (20) Nikolou, M.; Malliaras, G. G. *Chem. Rec.* **2008**, *8*, 13.
- (21) Ding, J.; Zhou, D.; Spinks, G.; Wallace, G.; Forsyth, S.; Forsyth, M.; MacFarlane, D. *Chem. Mater.* **2003**, *15*, 2392.
- (22) Lu, W.; Fadeev, A. G.; Qi, B. H.; Smela, E.; Mattes, B. R.; Ding, J.; Spinks, G. M.; Mazurkiewicz, J.; Zhou, D. Z.; Wallace, G. G.; MacFarlane, D. R.; Forsyth, S. A.; Forsyth, M. *Science* **2002**, *297*, 983.
- (23) Kaneto, K.; Kaneko, M.; Min, Y.; MacDiarmid, A. G. *Synth. Met.* **1995**, *71*, 2211.

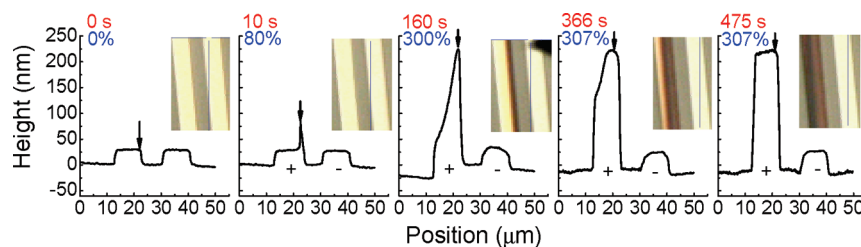


**Figure 1.** AFM height measurements and optical images (insets) of a 65 nm PEDOT:PSS film on a glass substrate covered with 30 nm gold electrodes ( $W = 1$  mm and  $L = 10$   $\mu\text{m}$ ) at different times after switching on a 4 V bias between the anode and cathode at 35% relative humidity. The relative height change is given.

ions and the subsequent uptake (or release) of water. This process is also called osmotic expansion.<sup>24,25</sup> Additively, changes in bond lengths and conformation in the polymer backbone may also contribute to expansion. Normally, in organic actuators, the insertion and deinsertion of ions is achieved while maintaining global electroneutrality; therefore, the polymer is either oxidized or reduced. Although in-plane actuation is commonly reported, remarkably few publications reported out-of-plane actuation. Smela et al.<sup>26,17</sup> measured a 1.5  $\mu\text{m}$  thick film of PPy with atomic force microscopy (AFM), showing an out-of-plane actuation of 125% at first cycle and 35% in normal cycle. The experiment was done in a  $\text{Na}^+\text{DBS}^-$ -rich solution. Recently, Kiefer et al.<sup>28</sup> reported a PEDOT bilayer in-plane actuator by electrochemical synthesis and obtained good lifetime performance. They showed a high deflection (1.5 mm) at a polymerization potential of 1.0 V and reasonable stability after 100 cycles. Out-of-plane actuation at ambient conditions of PEDOT:PSS thin films has not been reported.

In this paper, we show the large electrically induced height and volume changes in PEDOT:PSS thin films on gold electrodes in ambient air. Since no additional ionic electrolytes are used, the remarkable behavior cannot be straightforwardly mapped onto existing actuation models. To elucidate the possible mechanisms for this effect, we have performed a series of experiments that allow us to identify a predominantly reversible and a predominantly irreversible regime, for which tentative operational mechanisms are proposed in the Discussion section.

## 2. Results

**2.1. Height and Color Changes.** Figure 1 shows an example ( $L = 10$   $\mu\text{m}$ ) of the AFM topography and optical microscope images recorded for a 65 nm PEDOT:PSS film on a glass substrates covered with interdigitating gold electrodes (30 nm high, 10  $\mu\text{m}$  wide, spacing 10  $\mu\text{m}$ ) at different times after switching on a 4 V bias between the two electrodes. At 0 s, the PEDOT:PSS thin film covered the substrate where 30 nm thick gold electrodes were visible in AFM topography and the optical picture, since the PEDOT:PSS layer is

transparent. At 10 s, the anode showed a positive height change appearing from the channel side to  $\sim 84$  nm (or relative height change of  $\text{RHC} = 80\%$ <sup>29</sup>), while the PEDOT:PSS film remained transparent. At 160 s, the height change extended over the whole anode; the highest point was at 225 nm ( $\text{RHC} \approx 300\%$ ). The optical picture shows a dark front on the anode coinciding with a region of maximum height. At 366 s, the height and optical changes continued but saturated from the channel side. From 475 s onward, the height change stopped and a 230 nm ( $\text{RHC} \approx 307\%$ ) high plateau was formed on the anode exhibiting a brown color. A test sample was made to confirm that a fresh 250 nm thick film of PEDOT:PSS is not brownish but rather transparent light blue. The anode, kept at 0 V while the cathode was positively biased, remained entirely unchanged in color and topography for at least several hours. The height changes could be observed in a bias range from 4 to 10 V. Below 4 V, no height changes on the anode were observed; above 10 V, the thin film deteriorated quickly, showing bubbles which are likely to be associated with the fast electrolysis of water in the film. The clear fronts in height and color change that emerge for the channel side suggest that the mechanism involves transport of ions between the electrodes. The most abundant mobile ion in PEDOT:PSS (1:6) is the proton. The use of stiff cantilevers in tapping mode AFM assures that superficial water films do not significantly affect the measured topographies.

Under low sample illumination, a bluish color could be observed on the cathode for  $t < 100$  s while the anode was biased at 4 V, as shown in Figure 2. The bluish color appearing on the cathode indicates that PEDOT is reduced at the cathode.<sup>14,15</sup> In the neutral state, PEDOT exhibits a strong absorption in the red part of the spectrum at  $\sim 600$  nm and less at lower wavelengths, causing a bluish color. The disappearance of the bluish color at later times suggests that the reduced PEDOT is reacted away for  $t > 100$  s.

**2.2. Depletion and Morphology Changes in the Channel.** In section 2.1, the height above the anode was measured taking the channel as baseline.<sup>29</sup> To access the absolute height, a measurement of the height in the channel is necessary. The microstructure design of the interdigitating

(24) Bay, L.; Jacobsen, T.; Skaarup, S.; West, K. *J. Phys. Chem. B* **2001**, *105*, 8492.

(25) Velmurugu, Y.; Skaarup, S. *Ionics* **2005**, *11*, 370.

(26) Smela, E.; Gadegaard, N. *Adv. Mater.* **1999**, *11*, 953.

(27) Smela, E.; Gadegaard, N. *J. Phys. Chem. B* **2001**, *105*, 9395.

(28) Kiefer, R.; Weis, D. G.; Travas-Sejdic, J.; Urban, G.; Heinze, J. *Sens. Actuators, B: Chem.* **2007**, *123*, 379.

(29) Due to the absence of absolute baseline, the baseline was defined on the PEDOT:PSS surface around the positive electrode where the material was assumed not to completely deplete. This assumption enabled us to estimate the relative height change  $\text{RHC}(\%)$  as  $\text{RHC} = (A - T)/I$ , where  $A$  is the apparent height between the highest point above the anode and the lowest point on substrate,  $T$  is the electrode thickness, and  $I$  is the initial PEDOT:PSS film thickness.

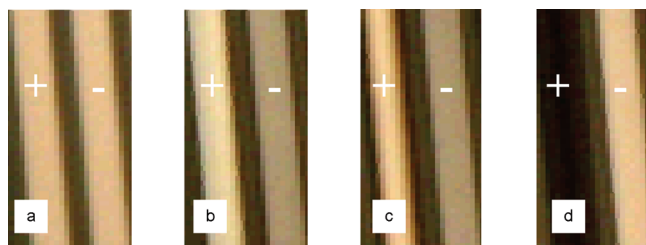


**Figure 2.** Optical microscope images of PEDOT:PSS films on two gold electrodes ( $W = 7$  mm and  $L = 4$   $\mu\text{m}$ ) taken at low sample illumination intensity. The cathode (right gold-colored bar) shows a bluish color for  $0 < t < 100$  s. The anode was biased at 4 V for (a) 0 s, (b) 59 s, (c) 78 s, and (d) 197 s, respectively.

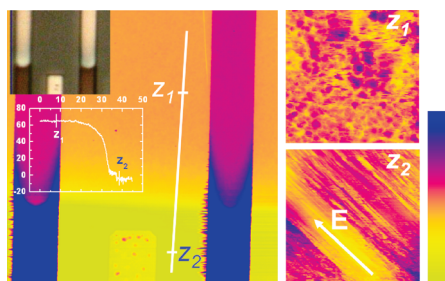


**Figure 3.** Left:  $50\text{ }\mu\text{m} \times 50\text{ }\mu\text{m}$  AFM height image ( $z_{\text{scale}} = 150$  nm) scanning two (left and right) biased anodes and one (middle) cathode. A 4 V bias was applied during 30 min. Top left inset: optical microscope image of the same area.  $z_1$  and  $z_2$  are placed in areas without and with electric field, respectively. A cross-section on the line through  $z_1$  and  $z_2$  is plotted in the inset with vertical axis in nanometers and horizontal axis in micrometers. On the right:  $400\text{ nm} \times 400\text{ nm}$  STM images ( $z_{\text{scale}} = 30$  nm) measured at  $z_1$  and  $z_2$ .  $z_1$  ( $z_2$ ) was taken with the following parameters: sample bias of 0.5 V (1.5 V), set point current of 500 fA (100 fA).

electrodes allowed us to measure the topography over areas with and without electric field in a single AFM measurement. Figure 3 shows a  $50\text{ }\mu\text{m} \times 50\text{ }\mu\text{m}$  AFM image scanning two (left and right) anodes and one (middle) cathode. Upon applying a bias over anode and cathode, an electric field will only be present where the two electrodes are interdigitating, i.e., in the lower part of the image, while in the upper part the field is absent. The top left inset represents an optical picture at the same scanning area, showing the electrodes and the (brown) material that has accumulated on the anodes next to the anode. Measurement positions  $z_1$  and  $z_2$  were placed in areas without electric field and with electric field, respectively.  $z_1$  was assumed to have an unchanged height and thickness. The line-section through  $z_1$  and  $z_2$  is plotted in the inset and is a proof of height diminution in the channel. The height difference between  $z_1$  and  $z_2$  is a direct reading of the depletion of material and is around 65 nm in the case of Figure 3. For very thin films, i.e., for 21 and 26 nm, the depletion measurements were not very accurate. In either case, the magnitude of the height change indicates that this is a bulk effect rather than a surface effect, acting on the thin (1–2 nm) PSS-enriched surface layer.

Besides AFM, also scanning tunneling microscopy (STM) measurements were performed to investigate the morphology of the PEDOT:PSS film. The top right panel of Figure 3 shows a  $400\text{ nm} \times 400\text{ nm}$  STM image of a pristine device (taken around point  $z_1$ , see above) revealing

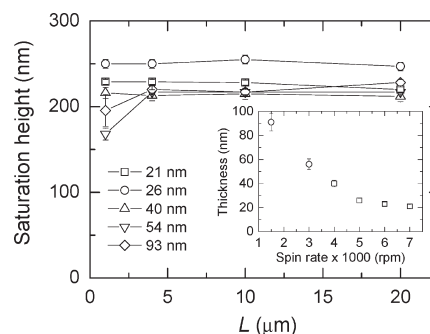


**Figure 4.** Maximum attainable height change (saturation) on the anode measured versus  $L$  for different film thicknesses  $d$ , see legend. The inset shows the film thicknesses versus the spin rate of deposition. Open squares are obtained from a diluted solution.

pancake-shaped domains, as reported previously.<sup>7</sup> The STM picture on the bottom right panel of Figure 3 was measured between the electrodes at  $z_2$ , after having applied the 4 V bias. The electric field orientation is indicated with the white arrow. The STM pictures show that the surface morphology in the channel changed from pancake shaped clusters to fibrous shapes in going from a pristine to a biased device. The fibrous orientation coincides with the electric field direction, indicating mass transport supported by the height reduction seen by AFM.

**2.3. Lack of Volume Conservation.** The AFM measurements in Figure 1 show that the final height of the anode after applying the bias equals 230 nm. Surprisingly, the maximum attainable height on the anode proved to be virtually independent of both channel length  $L$  and initial film thickness  $d$ , as shown in Figure 4. We attribute the nonsystematic, minor variation between layers of different thickness to differences in ambient humidity while measuring different samples. On a very wide anode (not shown), the height increase stopped after a certain length because the channel was depleted and the reaction that started at the anode edge stopped. A very wide cathode (not shown) did not change the maximum height on the anode.

This independence of the final height on  $d$  translates into very large RHC for very thin films, e.g.,  $\text{RHC} = 950\%$  for a 21 nm film. For these thinner films, the difference between anodic height increase and available material (in channel and cathode regions) can be as high as 150 nm. From this result, we conclude that a significant part of the height increase on the anode is not due to a rearrangement of material but due to a volume increase of the available material.

PEDOT:PSS films with a weight ratio of 1:20 (instead of the 1:6 used above) and with thicknesses of 42, 94, and 160 nm, respectively, gave maximum heights at  $245(\pm 5)$  nm,  $238(\pm 5)$  nm, and  $220(\pm 5)$  nm, i.e., mostly independent of film thickness. The absolute numbers are within experimental accuracy, the same for 1:6 and 1:20, suggesting that the height change is largely independent of the PEDOT:PSS composition. PEDOT:PSS films with a weight ratio of 1:1, however, did not show any height increase which we attribute to the much higher viscosity of this material. This stresses the fact that the effect in



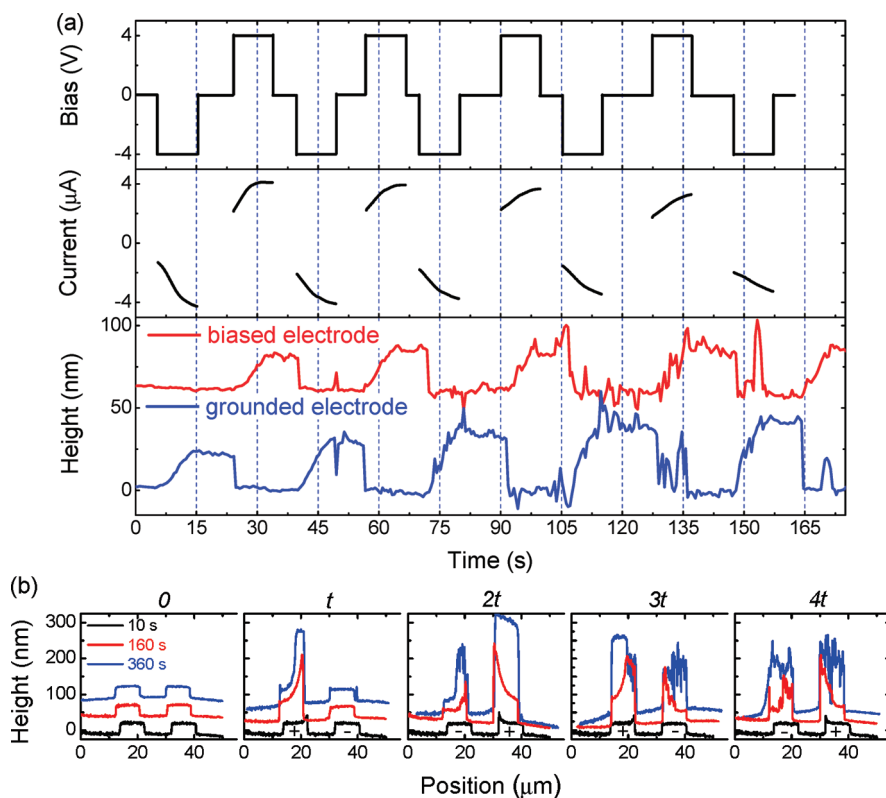


**Figure 5.** (a) A cyclic bias between +4 and -4 V was applied while the current and height above the electrodes were simultaneously measured versus time. When the bias is applied for  $t = 10$  s, the height change is reversible for five cycles. (b) Height traces for three different lengths of bias time  $t = 10$ , 160, and 366 s during the reversibility test. For clarity, the height traces are vertically shifted 25 nm from each other. The top horizontal axis shows the total bias time, which was switched in polarity after each  $t$ . The sign of the bias is indicated at the top of the panels.

terms of magnitude and dynamics of the height changes due to the electrochemical processes discussed below is also critically influenced by the mechanical properties of the film.

**2.4. Reversibility of the Height Change.** Because the observed height change is in part due to transport of material from the channel to the anode and in part due to a volume increase of the material at the anode, the reversibility of the processes is an interesting question.

Reversibility experiments were performed in a quantitative way; we used new devices under identical conditions (i.e., same batch,  $L$ ,  $W$ , and relative humidity) as those shown in Figure 1. When applying the bias for 10 s, height changes were found to be reasonably reversible for five full cycles (Figure 5a). We note that this reversibility excludes that the height change is due to electrolysis of water forming oxygen at the anode.<sup>17</sup> Moreover, the reversibility only applies to the height change but does not imply that the processes are electrochemically reversible in the sense that electron transfer between the electrode and the redox species occurs without significant energy barriers. In fact, the average rate for height increase was  $3 \text{ nm s}^{-1}$  ( $\sim 5\% \text{ s}^{-1}$ ) whereas the height decrease was significantly faster at  $-57 \text{ nm s}^{-1}$  ( $\sim 88\% \text{ s}^{-1}$ ) which demonstrates the absence of electrochemical reversibility. Under 0 V bias, the height change remained fully stable in time ranges of tens of seconds and partially stable up to several days, as discussed in the next section. The noisy AFM signal was mainly due to the fast changing topography although also some

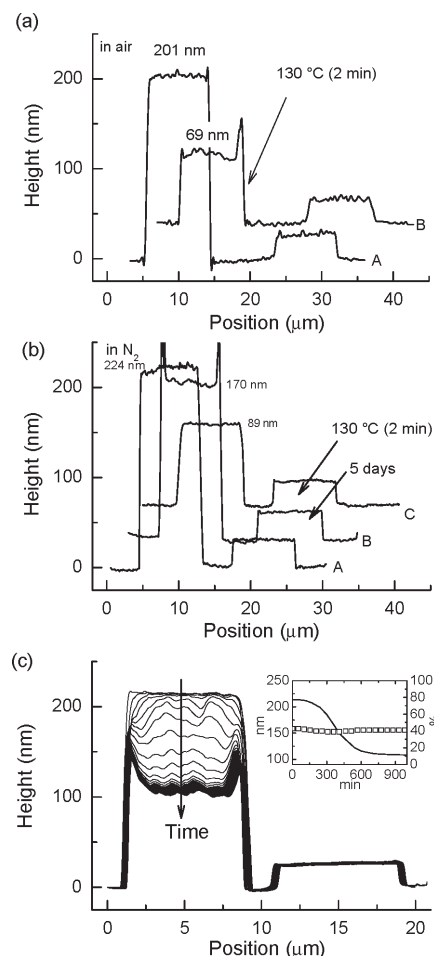
topographical spots appeared on the electrodes for higher cycle numbers.

Figure 5b shows the effect of applying a bias for a longer time (10, 160, and 366 s) in the reversibility experiments. Clearly, reversibility is reduced with increasing applied bias time: 10 s being largely reversible, 160 s being partially reversible, and 366 s being only marginally reversible. We remark that the irreversible height change is accompanied by the brownish color on the anode (Figure 1). This suggests that the reversible and irreversible processes are related to different processes, giving rise to different changes in the optical absorption. Recall also the bluish color on the cathode during the reversible height changes as discussed above.

### 2.5. Role of Humidity in Height Changes and Stability.

To investigate if the observed height and volume changes are associated with the uptake of water from the ambient, height changes were tested under different environmental conditions. We found that height changes were not observed in a dry  $\text{N}_2$  atmosphere and hardly observed in ambient air of reduced (13%) relative humidity.

To further assess the role of water, annealing experiments were performed using on layers in which a height change had been induced. In a first experiment, a layer was heated in air at  $130^\circ\text{C}$  for 2 min after being biased at 4 V to gain full height saturation. Representative height profiles before (line A) and after (line B) are shown in Figure 6a. The height dropped significantly from 201 to 69 nm, and a turquoise color appeared on the anode



**Figure 6.** Relaxation experiments by annealing in (a) ambient air and (b) N<sub>2</sub> and by time in (c) air of PEDOT:PSS layers in which a height change had been induced previously in ambient air. Curves in panel (c) were recorded every 60 min during 4 days. The inset shows the height in nanometers (continuous curve) in the middle of the anode and the relative humidity in ambient air in percent (open squares) versus time.

instead of the original brown. The original height of the anode prior to applying a bias was 30 nm, whereas the height at the end of the experiment was ca. 69 nm, indicating that the height gain is only partly undone by annealing.

In a second experiment, a layer that was biased at 4 V to gain full height saturation was transported to and left in a glovebox filled with dry N<sub>2</sub> for 5 days (Figure 6b). The height dropped from 224 to 170 nm. A subsequent heating step at 130 °C for 2 min (line C) caused an additional height loss to 89 nm, the same height that was found by annealing in air.

The absence of height changes in dry environments already indicated that ambient water is involved, either directly by enabling electrochemical reactions or indirectly by acting as a plasticizer for PEDOT:PSS. The very similar effects of slow and forced drying, i.e., a height reduction of the PEDOT:PSS layer on the anode while the cathode remains unchanged, suggest that a significant fraction (~60%) of the gained height is due to hygroscopic effects, i.e., absorbed water. The material remaining on the anode after evaporation of excess water has

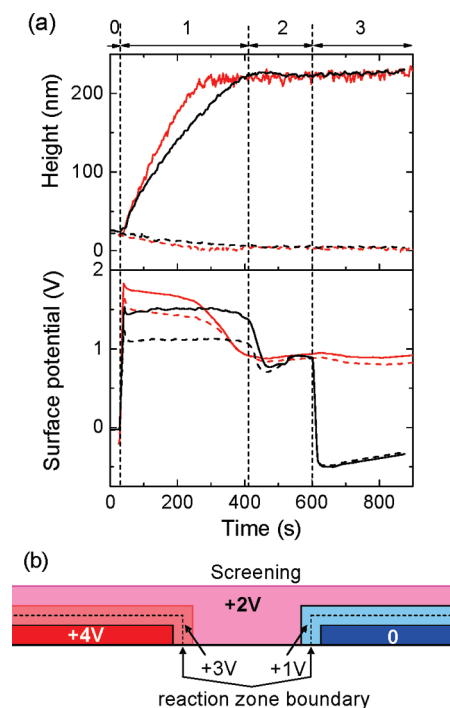


**Figure 7.** (a) A 21 nm PEDOT:PSS film was measured at 59% relative humidity with SKPM at 0 nm lift height (black lines). In regions 1 and 2 (indicated on the upper *x*-axis), a 4 V bias was applied, while in regions 0 and 3 both electrodes were grounded. SKPM and height measurements are shown versus time simultaneously on the anode (solid line) and cathode (dashed line). For comparison, a 91 nm PEDOT:PSS film (red lines) was measured under the same conditions. (b) Schematic drawing of the potential inside the PEDOT:PSS thin film with anode and cathode at 4 and 0 V, respectively. The potential drops in the light blue and light red colored regions.

likely been transported from the channel and cathode, as discussed in section 2.2 above.

A third experiment involved the continuous height measurement in ambient air during 4 days (Figure 6c). The inset shows the height (continuous curve) in the middle of the anode versus time. In addition to a drop of height by 100 nm over 4 days, a color change from brownish to turquoise was observed. The characteristic “ears” seen to develop in Figure 6c are reminiscent of the coffee stain effect, suggesting some material transport to the edges of the elevated regions where enhanced evaporation of water can be expected.

**2.6. Surface Potential Measurements.** Scanning Kelvin probe microscopy (SKPM) measurements were performed on different PEDOT:PSS films. Typical results for a layer with initial film thickness of 21 nm are shown in Figure 7a (black lines). Figure 7a shows the simultaneously measured height (continuous line) and surface potential averaged over the anode (continuous line) and cathode (dotted line) versus time. In regions 1 and 2, a 4 V bias is applied, while in regions 0 and 3, both electrodes are grounded. Surprisingly, the surface potential of both electrodes is roughly equal ( $V_{\text{anode}} - V_{\text{cathode}} \approx 0.4$  V) despite a bias voltage of 4 V between them (region 1 in Figure 7a). Once saturation is reached (at  $t = 413$  s, region 2), a relatively sudden drop of both surface potentials is observed. PEDOT:PSS films with a thickness of 65 nm (not shown) and 91 nm (red lines) exhibited similar surface potential behavior, though

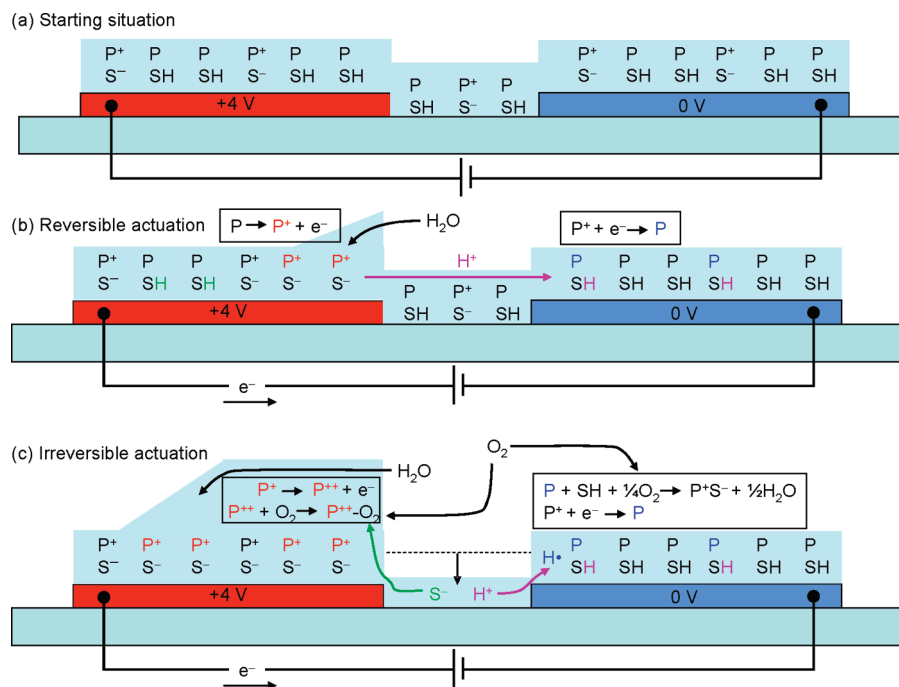


**Figure 8.** Schematic drawings of starting situation (a), reversible (b), and irreversible (c) height changes. Repeating units of PEDOT<sup>+</sup> and PSS<sup>-</sup> are represented by P<sup>+</sup> and S<sup>-</sup>. Redox reactions occurring are represented in the boxes. (a) The starting situation reflects that in pristine PEDOT:PSS about 1 in 3 PEDOT monomer units is oxidized and electrostatically bound to PSS<sup>-</sup>. (b) During reversible height change, P units are oxidized at the anode (red) and P<sup>+</sup> units are reduced at the cathode (blue), accompanied by H<sup>+</sup> transport (from left to right). This reaction will become limited by the availability of P (or P<sup>+</sup>) at the electrodes and the imbalance in H<sup>+</sup> concentration. (c) Irreversible height change will occur by overoxidation of PEDOT (denoted with P<sup>2+</sup>) followed by addition of O<sub>2</sub>, while remaining PSS<sup>-</sup> ions in the channel will move. During the entire height change (b and c), water is absorbed from the ambient, causing the height change not to be limited by the amount of starting material in the channel.

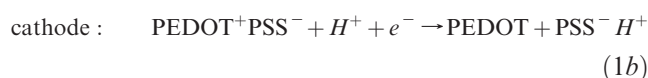
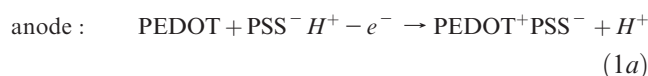
with a significantly smaller difference of surface potentials between the electrodes ( $V_{\text{anode}} - V_{\text{cathode}} \approx 0.2$  V) in region 1, i.e., while applying a bias.

The fact that only a fraction of the applied bias is visible in the surface potential is attributed to (partial) electrostatic screening by mobile ions present in the PEDOT:PSS, as illustrated in the cartoon in Figure 7b. An interpretation of these observations in terms of material degradation can be ruled out as it is also observed at low (< 4 V) bias and short times when degradation does not (yet) take place. The smaller difference between anodic and cathodic surface potentials for thicker (65 and 91 nm) films strongly suggests that the screening length is on the order of a few tens of nanometers. We note that Taylor et al.<sup>30</sup> reported similar electrostatic screening in PEDOT:PSS, though on longer channels.

### 3. Discussion

Before discussing the electrochemistry, it should be pointed out that the conducted experiments are essentially two-terminal; hence, no reference potential exists like in, e.g., electrochemical cells. From the observations above, it is clear that at least two different mechanisms are relevant: one reversible reaction causing a bluish color on the cathode preceding one or more irreversible reactions causing the occurrence of dark colors on the anode. For the reversible reactions, we propose the following electrochemical

redox reactions, considering that a spin coated, pristine, PEDOT:PSS film is in fact partially oxidized:



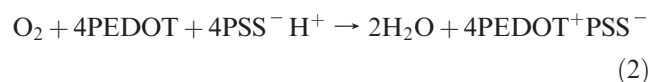
where PEDOT<sup>+</sup>, PSS<sup>-</sup>, and H<sup>+</sup> represent, respectively, a neutral (oxidized) PEDOT repeat unit, the neutral (reduced) PSS repeat unit, and the proton. Starting from a spin coated PEDOT:PSS as drawn in Figure 8a and under high enough bias, further oxidation at the anode causes the remaining neutral PEDOT repeat units to form PEDOT<sup>+</sup>PSS<sup>-</sup> in a higher oxidation state, liberating H<sup>+</sup>. To maintain charge neutrality and a current, the excess protons formed on the anode can be most easily transferred to the cathode through the PEDOT:PSS layer under the influence of the electric field between anode and cathode. The excess of PSSH in the 1:6 wt ratio PEDOT:PSS and the presence of water (up to 25% in ambient conditions<sup>9</sup>) mediate the transport of the small H<sup>+</sup> ion via the Grotthuss mechanism,<sup>31</sup> by which the hydronium species (H<sub>3</sub>O<sup>+</sup>) shuttles a proton to a neighboring water molecule, resulting in a proton mobility that is considerably larger than that of other similar cations. Alternatively, H<sub>3</sub>O<sup>+</sup> ions could migrate, which does not fundamentally change reactions. Due to the

(30) Taylor, D. M.; Morris, D.; Cambridge, J. A. *Appl. Phys. Lett.* **2004**, *85*, 5266.

(31) Agmon, N. *Chem. Phys. Lett.* **1995**, *244*, 456.

bulkiness of hydronium ions as compared to protons, this process is expected to be much slower than proton transport. In section 2.5, we showed that dry conditions indeed prevent the electrically induced height change effect. Due to their much larger size, the ion mobilities of PEDOT<sup>+</sup> to the cathode or PSS<sup>-</sup> to the anode will be less.

Reaction 1b is the electrochemical reduction of PEDOT<sup>+</sup>, the reverse of reaction 1a, and is proposed to occur at the cathode. The proton is supplied by the anodic reaction and forms PSSH with PSS<sup>-</sup>, while PEDOT<sup>+</sup> is (partially) reduced to PEDOT. The observation of a bluish color on the cathode (section 2.1, Figure 2) confirms this reduction step for times when  $t < 100$  s. For longer times, the working conditions enable the oxidation of PEDOT by oxygen from the air:



which would explain the observed suppression of the bluish color on the cathode for times when  $t > 100$  s.

The increased height of the PEDOT:PSS film on the anode observed when applying a positive bias may be caused by (a) a mass transport of anions coming from the cathode, i.e., electromigration, (b) conformational changes, or (c) osmosis, i.e., uptake of H<sub>2</sub>O from ambient air or other parts of the film. The proposed redox reactions 1a and 1b, however, do not involve anionic species to transport charge from the cathode toward the anode. Doping of polymer chains is known to induce conformational changes. X-ray measurements on highly oriented polyacetylene showed a chain length elongation (or contraction) upon Li<sup>+</sup> and K<sup>+</sup> donor (or I<sup>-</sup> acceptor) doping.<sup>32</sup> However, the reported effects are typically small as compared to the height changes observed here. Hence, in our view, neither ion transport nor conformational changes can explain the changes on the anode. Therefore, we suggest an osmotic mechanism<sup>24,25,27</sup> to explain the height change and, simultaneously, the apparent lack of volume conservation discussed in section 2.3. Reaction 1a leads to an increased positive doping of PEDOT<sup>+</sup> chains at the anode, causing the further uptake of ambient H<sub>2</sub>O. Alternatively, other parts of the thin film may act as source for H<sub>2</sub>O. The assignment of H<sub>2</sub>O uptake on the anode as the main cause of volume increase is in full agreement with the observations described in section 2.5. Moreover, it is in line with the interpretation of similar data on doped PPy.<sup>24,26,27</sup> We note that the devices of refs 26 and 27 were submerged in an electrolyte solution that can act as a water reservoir, whereas in the present case ambient air and other parts of the film act as reservoirs.

An upper limit to the amount of absorbed water can be calculated as height increase  $\times$  electrode width  $\times$  electrode length, i.e.,  $0.2 \times 10 \times 1000 = 2 \times 10^3 \mu\text{m}^3$  per anode. This water can be directly absorbed at the anode, or more likely, it is extracted from the surrounding (humid) film, which

then re-establishes its equilibrium with the ambient air by absorbing water. The latter process effectively enhances the absorbing area.

By changing the bias polarity, reactions 1a, and 1b swap electrode, and the PEDOT<sup>+</sup> concentration on the “new” anode increases at the cost of the concentration on the “old” anode. Hence, an osmotic driving force for H<sub>2</sub>O transport from the old to the new anode develops, making the height change reversible, as shown for short bias times in Figure 5. A schematic drawing of the reversible process is shown in Figure 8b.

Further confirmation for the osmotic scenario in the reversible regime comes from the observed asymmetry in the height change rate upon oxidation and reduction (Figure 5a). It was observed by Efimov et al. that the mass increase of a PEDOT film upon oxidation in an electrolyte solution is considerably slower than the mass loss upon reduction.<sup>33</sup> This effect was attributed to slow water exchange upon oxidation, in line with the present observations and interpretation.

When the PEDOT becomes fully neutralized at the cathode or fully oxidized at the anode, reactions 1b and 1a will terminate and irreversible reactions start. At present, the irreversible regime is only partly understood and we can only speculate on the exact causes. In view of the color changes observed (Figure 1b), the most likely irreversible reaction occurring on the anode is overoxidation of PEDOT, which is known to occur at large anodic potentials in a humid environment.<sup>34</sup> Overoxidation leads to a strong reduction of the conductivity and occurs as a two-stage process, consistent with the double color change discussed in section 2.1. It has been reported that during the first stage of overoxidation nucleophiles (e.g., water or oxygen) are reversibly substituted on the 3 or 4 positions of the thiophene units; in the second stage, irreversible formation of SO<sub>2</sub> or COOH moieties occurs.<sup>34</sup>

During the overoxidation, further migration of ions must occur. The remaining height after drying and/or annealing (Figure 6), the significant layer thickness decrease in the channel, and the morphological changes in the channel (Figure 3) prove that a substantial amount of material must have been moved from the channel region to the anode. This basically leaves transport of PSS<sup>-</sup> as only option, as schematically shown in Figure 8c. It is surprising that such a large molecule is sufficiently mobile, although the presence of  $\sim 25\%$  of water in the film may have a significant plasticizing effect. In this regime, the height increase would then be a combination of mass (PSS) transport, uptake of water (osmosis), and possibly binding of oxygen. After reaching the maximum attainable height, the experiments in section 2.2 clearly showed a partly depleted channel with an orientation of the remaining material in the field direction, consistent with the idea that the channel acts as a source of PSS<sup>-</sup>. The

(32) Murthy, N. S.; Shacklette, L. W.; Baughman, R. H. *J. Chem. Phys.* **1987**, *87*, 2346.

(33) Efimov, I.; Winkels, S.; Schultze, J. W. *J. Electroanal. Chem.* **2001**, *499*, 169.

(34) See: Tehrani, P.; Kancierzewska, A.; Crispin, X.; Robinson, N. D.; Fahlman, M.; Berggren, M. *Solid State Ionics* **2007**, *177*, 3521 and references therein.



thermal and temporal relaxation experiments (section 2.5) show a partial height reduction reflecting the  $\text{H}_2\text{O}$  component; the remaining material on the anode is, therefore, attributed to PSS and possibly incorporated oxygen. From the absence of any color changes on the cathode, it seems likely that the required reduction step on the cathode during PEDOT overoxidation is still reaction 1b, in combination with reaction 2.

The tentative mechanisms sketched above rationalize most observations, but the independence of the maximally attainable height on channel length and film thickness and on PEDOT:PSS ratio (section 2.3) remain to be explained. The answer to these, at first sight, surprising independencies comes from the SKPM experiments (section 2.6). The thickness dependence of the surface potential screening indicates that the screening length is on the order of tens of nanometers. Consequently, only a very thin (tens of nanometers) region is at sufficiently large voltage with respect to the rest of the sample to enable electrochemical reactions (Figure. 7b). Hence, only the reactive material on the anode within the screening length can react. In other words, the screening length rather than the film thickness determines the maximum increase in height. For the same reason, the height change only occurs on top of the electrode and does not progress in the channel. A similar reasoning explains the channel length independence: as long as the amount of material within the screening length is the limiting factor, the final height is independent of  $L$ . Only for short channels, the combined amount of material in the channel and on the cathode may become limiting, as seems to happen in a few instances in Figure 4. The PEDOT:PSS ratio independence might be explained by a considering that the most likely screening species are the mobile protons. Since PSS is present in similar absolute concentrations in 1:20 and 1:6 PEDOT:PSS material and is the proton source, both compositions will have similar screening lengths. Since the amount of PEDOT within the screening length is lower for 1:20, one might expect less height change for 1:20. However, other effects like viscosity, as is the case for 1:1, will play a role as well.

#### 4. Conclusion

In conclusion, we have found an unexpected large electrically induced height and volume change of PEDOT:PSS thin films on gold electrodes under ambient conditions. The maximum attainable height increase was found to be independent of film thickness and can reach a relative height change of 950% for a 21 nm thick film in the first cycle. On basis of a wide range of experiments, we propose a qualitative electrochemical model that assumes a reversible regime in which proton transport is dominant and an irreversible regime in which overoxidation of PEDOT occurs and  $\text{PSS}^-$  transport dominates. In both regimes, osmotic water absorption

is responsible for a large fraction of the volume expansion. The height changes under influence of electrical bias may be useful in low-cost actuator-like applications operating under ambient conditions or bias-controlled microlenses.

#### 5. Experimental Section

In total, 20 substrates, each containing 62 microstructured pairs of interdigitated electrodes were made. Both anode (positive) and cathode (negative) were  $10\ \mu\text{m}$  wide, the distance  $L$  separating the electrodes was 1, 4, 10, or  $20\ \mu\text{m}$ , whereas the channel width  $W$  was 1, 7, or 19 mm. Glass substrates and Si/ $\text{SiO}_2$  wafers did not show different results. The samples were manufactured using standard UV photolithography. Starting from chemically cleaned substrates, 5 nm of Ti as adhesion layer and 25 nm of Au were subsequently deposited on the developed photoresist by electron beam evaporation under high vacuum conditions. A classical lift-off with acetone was done to remove the resist and to reveal the microstructures.

In our experiments, PEDOT:PSS with a weight ratio of 1:6 was purchased from H. C. Starck (Baytron P VP Al 4083, recently renamed Clevios P Jet (OLED)). Prior to spin coating, 2 mL of PEDOT:PSS was taken in a syringe and filtered through a  $5\ \mu\text{m}$  porous material (Schleicher & Schue, FP 30/5,0 CN-S). Film thickness was varied by adjusting the spin rate and dilution, as shown in the inset of Figure 4. The samples were annealed at  $200\ ^\circ\text{C}$  for 2 min in order to reduce water content and create a compact layer. Film thicknesses were measured with a profilometer or an AFM. The measured thicknesses varied 5 nm depending on the sample location. Other PEDOT:PSS compositions 1: $x$  were used with  $x = 1$  and  $x = 20$ . The high viscosity of  $x = 1$  did not allow filtering through porous material. For  $x = 1$ , no height change was observed. Between fabrication and measurement, the samples were stored in a vacuum glass container ( $10^{-2}$  mbar) or in a  $\text{N}_2$ -filled glovebox.

The AFM (and scanning Kelvin probe microscope, SKPM) was performed under ambient conditions with a Veeco Dimension 3100. Free software (Super Screen Recorder, version 2.0) was used to capture optical images from the built-in camera as a video file. We used Nanosensors tips (PPP-NCHR-50, 330 kHz resonance frequency and  $\sim 42\ \text{N m}^{-1}$  spring constant) for AFM and Pt-coated Olympus tips (OMCL-AC240TM-B2, 70 kHz resonance frequency and  $\sim 2\ \text{N/m}$  spring constant) for SKPM. The scanning tunneling microscope (STM) was a Veeco Multi-mode equipped with a low current preamp and was operated under ambient conditions. The STM tips were cut from Pt/Ir wire. Current–voltage characteristics were measured using a Keithley 4200 parameter analyzer, which was also used to provide biases and measure currents during scanning probe experiments.

**Acknowledgment.** We are very grateful to Dr. Margreet de Kok, Dr. Paul van Hal, and Dr. Bea Langeveld for materials supply and to Dr. Klára Maturová and Mr. Lukas Brinek for technical assistance. We thank the COBRA Research Institute for assistance with micropatterning. The work of D.S.H.C. is made possible by a NanoNed grant (NanoNed is the Dutch nanotechnology initiative by the Ministry of Economic Affairs).